

Experimental implementation of non-Gaussian attacks on a continuous-variable quantum key distribution system

Jérôme Lodewyck,^{1,2} Thierry Debuisschert,¹ Raúl García-Patrón,³
Rosa Tualle-Brouri,² Nicolas J. Cerf,³ and Philippe Grangier²

¹*Thales Research and Technologies, RD 128, 91767 Palaiseau Cedex, France*

²*Laboratoire Charles Fabry de l'Institut d'Optique, CNRS UMR 8501,
Campus Universitaire, bât 503, 91403 Orsay Cedex, France*

³*QuIC, École Polytechnique, CP 165, Université Libre de Bruxelles, 1050 Bruxelles, Belgium*

An intercept-resend attack on a continuous-variable quantum key distribution protocol is investigated experimentally. By varying the interception fraction, one can implement a family of attacks where the eavesdropper totally controls the channel parameters. In general, such attacks add excess noise in the channel, and may also result in non-Gaussian output distributions. We implement and characterize the measurements needed to detect these attacks, and evaluate experimentally the information rates available to the legitimate users and the eavesdropper. The results are consistent with the optimality of Gaussian attacks resulting from the security proofs.

PACS numbers: 03.67.Dd, 42.50.Lc, 42.81.-i, 03.65.Ud

Quantum key distribution (QKD) enables two distant parties – Alice and Bob – linked by a quantum channel and an authenticated classical channel to share a common secret key that is unknown to a potential eavesdropper Eve. For this purpose, Alice and Bob have to agree on a proper set of non-commuting quantum variables, as well as a proper encoding of the key into these variables. Common QKD setups use so-called discrete variables (e.g. the polarization of a photon), thereby requiring single-photon sources or detectors [1].

In this Letter, we shall rather follow an alternative procedure, pioneered in [2, 3], which consists in encoding the key into continuous variables (CV). Specifically, we use a CVQKD protocol with coherent states introduced in [4]. The action of a possible eavesdropper then appears as *added noise* on the observed continuous data. More precisely, line losses correspond to a restricted class of attacks, often called beam-splitting attacks, which only add Gaussian “vacuum” noise. Other attacks typically add more noise, called “excess noise”, which may be non-Gaussian. It is generally crucial to show that Alice and Bob can measure these noises with the required accuracy in order to ensure the security of CV-QKD.

In order to analyse these noises, we have explicitly implemented several non-trivial actions of the eavesdropper Eve, which are simple but general enough to include both Gaussian and non-Gaussian features. These attacks are implemented optically as partial intercept-resend (IR) operations, in which the signal beam is either measured and subsequently re-prepared, or is eavesdropped using a beam splitter (BS). These attacks enable Eve to control independently the two main channel parameters, namely the loss (BS part) and excess noise (IR part), simply by adjusting the intercepted fraction. They are therefore much more powerful than a simple BS attack corresponding to a pure line loss. We examine in detail how well Alice and Bob can detect them in real operating condi-

tions. The experiment confirms and emphasizes that it is crucial to properly evaluate the channel excess noise in order to warrant the security of the present CV-QKD protocol [4, 5, 6]. In addition, we explicitly measure the information gained by Eve for a wide range of partial IR attacks, and check that it never exceeds the bound based on Gaussian attacks (with excess noise). This is in full agreement with the security proof given in [7].

Our CV-QKD protocol is based on coherent states and reverse reconciliation, as described in [4]. Alice sends Bob a train of coherent states $|x + ip\rangle$ where the quadratures (x, p) are randomly chosen from a bivariate Gaussian distribution with variance V_A . Bob randomly measures either x or p , and publicly announces his choice. A binary secret key is then extracted from the correlated continuous data by using a sliced reconciliation algorithm [8, 9]. This protocol is well suited for practical QKD because it only requires conventional fast telecommunication components, such as InGaAs photodiodes or electro-optics modulators. A full QKD setup with a typical repetition rate of 1 MHz can be assembled with off-the-shelves components [10]. The security of the protocol is proven against a wide range of attacks, namely Gaussian individual attacks [4], finite-size non-Gaussian attacks [7], and Gaussian collective attacks [11, 12]. It will be sufficient for our needs here to focus on the proof of [7], which provides a simple analytical expression for the secret key rates against non-Gaussian attacks.

General framework. The processing of a coherent state via a Gaussian quantum channel can be described as follows. Its amplitude is multiplied by \sqrt{T} , where $T \leq 1$ is the channel transmission, while its noise variance is increased to $(1 + T\epsilon)N_0$ at the output, where N_0 stands for the shot-noise level and ϵ is the so-called excess noise (referred to the input). Assuming that the limited efficiency $\eta < 1$ of the homodyne detector deteriorates Bob’s reception but does not contribute to Eve’s

information (so-called “realistic mode” in [4, 10]), the information rates can be written as

$$I_{AB} = \frac{1}{2} \log_2 \frac{\eta T V_A + 1 + \eta T \epsilon}{1 + \eta T \epsilon} \quad (1)$$

$$I_{BE} = \frac{1}{2} \log_2 \frac{\eta T V_A + 1 + \eta T \epsilon}{\eta / \left[1 - T + T \epsilon + \frac{T}{V_A + 1} \right] + 1 - \eta} \quad (2)$$

In reverse reconciliation [4], the secret key rate is given by $K = \beta I_{AB} - I_{BE}$, where β is the efficiency of the reconciliation algorithm with respect to Shannon’s limit. All the quantities appearing in these formulas are known or can be measured by Alice and Bob. In practice, Alice and Bob must carefully evaluate T and ϵ in order to infer the optimal attack Eve can perform, and therefore to upper bound I_{BE} . This is done by statistical evaluation over a random subset of the raw data [10].

Non-Gaussian attacks. Let us consider a particular non-Gaussian attack, namely a partial intercept-resend (IR) attack: Eve detects and resends a fraction μ of the pulses, while she performs a standard beam-splitter (BS) attack on the remaining fraction $(1 - \mu)$. For the IR step, Eve performs a simultaneous measurement of both quadratures (Fig. 1), and resends a coherent state displaced according to her measurement results. For the BS step, Eve is assumed to keep the tapped signal in a quantum memory and to measure it only after Bob has revealed his measurement basis. For given channel parameters (T, ϵ) , the optimal attack is known to be Gaussian [7]. It can be achieved using an “entangling cloner” [5], which simply reduces to a BS attack if $\epsilon = 0$. If $\epsilon \neq 0$, the partial IR attack that we consider here is not optimal, although it has several advantages for our demonstration purposes. First, it gives Eve a very simple way to exploit the excess noise of the line in order to gain more information; second, it provides the opportunity to check explicitly the bound on Eve’s information for non-Gaussian attacks, deduced from Alice and Bob’s noise variance measurements as established in [7].

Let us emphasize that for a full IR attack ($\mu = 1$), one has $\epsilon = 2$. This corresponds to the “entanglement breaking” limit in our protocol [5, 13], at the edge between the classical and quantum regimes. No entanglement can be transmitted through the quantum channel, and therefore no secret key can be extracted. For a lossy channel, this added noise gets attenuated, so the entanglement breaking limit may become difficult for Bob to detect. Thus, as another challenge to our experimental implementation, it is interesting to check whether Bob can detect this IR attack and properly reject the transmitted key.

Experimental setup. We have realized the IR attack using the device described Fig. 2. It is a coherent-state QKD setup, working at 1550 nm and exclusively assembled with fiber optics and fast telecom components. It displaces a train of pulsed coherent states within the complex plane, with arbitrary amplitude and phase, ran-

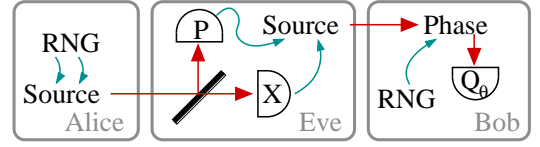


FIG. 1: Intercept-resend attack. Alice prepares a random coherent state, and Bob chooses a random quadrature measurement with a random number generator (RNG). In between, Eve makes an heterodyne measurement of each incoming quantum state, and displaces another generated coherent state according to her measurement result.

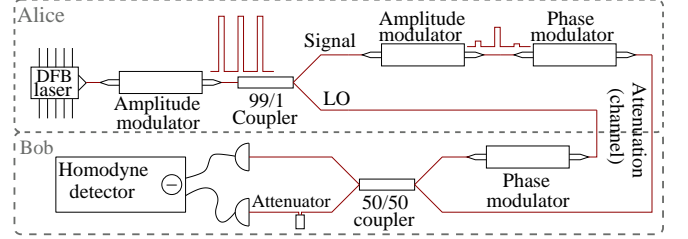


FIG. 2: Experimental setup. Alice generates modulated signal pulses. Bob measures a random quadrature with a pulsed, shot noise limited homodyne detector.

domly chosen from a two-dimensional Gaussian distribution with variances $V_A = 36.6 N_0$. The pulse width is 100 ns. The signal is sent to Bob along with a strong phase reference – or local oscillator (LO), with 10^9 photons per pulse. Bob selects an arbitrary measurement phase with a phase modulator placed on the LO path. The selected quadrature is measured with an all-fiber shot noise limited, time-resolved homodyne detector. A key transmission is composed of independent blocks of 50000 pulses, sent at a rate of 500 kHz, among which 10000 test pulses with agreed amplitude and phase are used to synchronize Alice and Bob and to determine the relative phase between the signal and LO (see [10] for more details). Knowing this relative phase, Bob is able to choose an absolute phase measurement, for example one of the field quadratures x and p , with a software control loop.

Practical QKD requires that only a part of the dataset is revealed for channel parameters evaluation. This finite set size introduces statistical fluctuations that can alter the excess noise estimate. Therefore, security margins have to be considered when computing information rates. In all the experimental curves shown below, the number of sampling points for channel characterization has arbitrarily been chosen to be 5000 (i.e. 13% of the 40000 available pulses) for illustration purpose, and may be optimized for each value of the channel transmission.

Implementation of full IR attacks. To implement an IR attack as in Fig. 1, one would need three homodyne detectors and two modulation setups. To avoid unneces-

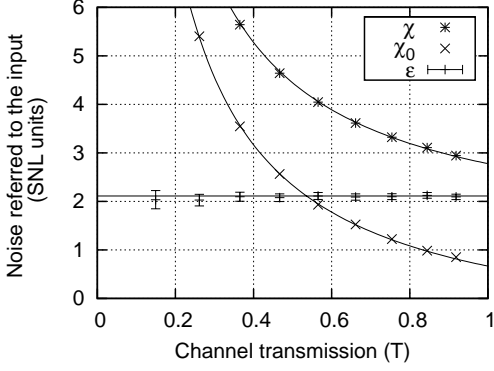


FIG. 3: Variance of the noise measured by Bob that is produced by a full IR attack ($\mu = 1$). We define the total added noise (referred to the input) as $\chi = \chi_0 + \epsilon$, with $\chi_0 = 1/(\eta T) - 1$ denoting the loss-induced vacuum noise and ϵ denoting the excess noise. The total added noise χ (stars) is measured experimentally, while χ_0 (crosses) is deduced from the measured transmission (T) and from Bob's homodyne efficiency ($\eta = 0.6$). Then ϵ (plus) is obtained from their difference. The uncertainties margins on ϵ represent the standard deviation of statistical fluctuations when computing over a finite data subset (5000 points out of 40000).

sary hardware duplication, this attack has been split in three phases, with the role of Eve being played either by Alice or by Bob. First, Alice sends coherent states, and Bob simulates Eve measuring the x quadrature of the incoming states. Then, the same operation is repeated with a p measurement. To take into account Eve's beam splitter shown in Fig. 1, the variance measured by Eve (actually Bob) is adjusted to be exactly half of Alice's output modulation. This calibration also virtually includes the losses within the homodyne detector into the beam splitter, thus simulating a perfect heterodyne measurement. Both x and p measurement outputs are then communicated to Alice through a classical channel so that she can simulate Eve resending coherent states that are displaced accordingly. After this sequence, the correlations between Alice and Bob are measured in order to determine the channel parameters. Since Alice and Eve drop the quadrature not measured by Bob, our two-step implementation of the interception is legitimate.

The excess noise referred to the channel input is measured by Bob for different channel transmissions, selected with an amplitude modulator. For a full IR attack ($\mu = 1$), the excess noise is measured to be about $0.1 N_0$ above the expected $2 N_0$ entanglement breaking bound (Fig. 3). This is due to the various technical noises encountered throughout the IR process, which can be independently determined from the experimental data (mostly laser phase noise and modulation imperfections). Since this technical noise is quite small, we also conclude that the imperfections related to the method used to "simulate" Eve are negligible.

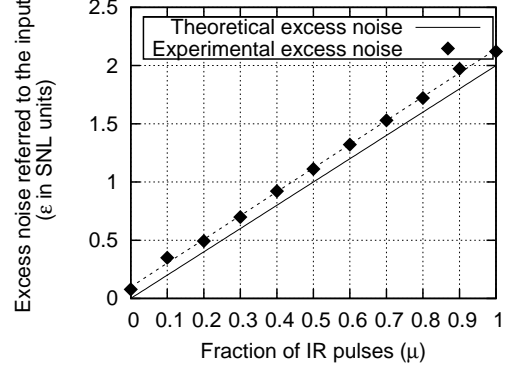


FIG. 4: Variance of the excess noise in a partial IR attack. Each point results from an average of the measured excess noise for different channel transmissions (see the ϵ vs. T plot of Fig. 3). The solid line plots the expected excess noise due to an IR attack on a fraction μ of the pulses. Due to technical noise, the experimental data are above this line, typically less than $0.1 N_0$ (dashed line).

Implementation of partial IR attacks. Because the full IR attack reaches the entanglement breaking limit, it is not the best for Eve to tap information from the quantum channel. As explained previously, a more subtle way for Eve to interact is to intercept and resend only a fraction μ of the pulses, and to implement a BS attack on the rest of the pulses. In this case, Eve can choose the amount of noise she wants to introduce independently of the channel transmission. This allows a complete channel parameter control, which is not achievable with a simple BS attack ($\epsilon = 0$) nor with an IR attack where the added noise is fixed for a given channel transmission.

An important point is that the probability distribution of Bob's measurements becomes the weighted sum of two Gaussian distributions with different variances, namely $TV_A + N_0$ for the transmitted data (BS) and $T(V_A + 2N_0) + N_0$ for the resent data (IR), so the attack is not Gaussian any more. Figure 4 shows the measured excess noise for different interception fractions μ . Ideally, it is given by the weighted sum of the excess noises in the IR and BS cases, *i.e.*, $\epsilon_{\text{TOT}} = \mu \epsilon_{\text{IR}} + (1 - \mu) \epsilon_{\text{BS}} = 2\mu$. In our experiment, we have to add the technical noise of variance $\epsilon_T = 0.1 N_0$, which leads to $\epsilon_{\text{TOT}} = 2\mu + \epsilon_T$, in good agreement with the experimental data.

For such an attack, the achievable secret key rate is lower bounded by the information rate for an equivalent Gaussian attack characterized by the same variance and conditional variance of the data distribution [7]. The Gaussian mutual information rate I_{AB}^g between Alice and Bob can be derived from the noise variance measurements with a Gaussian channel model characterized by the same correlations. This can be compared with the actual mutual information rate I_{AB}^{ng} computed from the measured data distribution in presence of the partial IR attack.

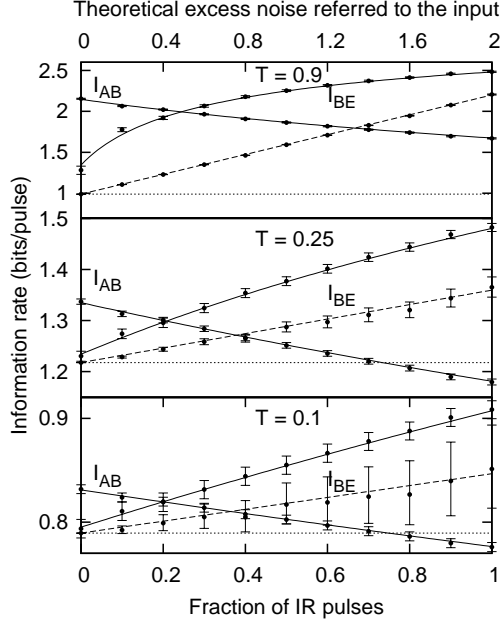


FIG. 5: Mutual information rates for a non-Gaussian partial IR attack, for $T = 0.1, 0.25$ and 0.9 , with $V_A = 36.6 N_0$, $\eta = 0.6$ and a technical excess noise of $0.1 N_0$. The mutual information I_{BE} is plotted for a Gaussian model with equivalent excess noise (solid lines), as well as for a BS attack (dotted lines), and for a partial IR attack (dashed lines). It is compared with the Gaussian mutual information I_{AB} . As expected, the IR attack enables to exploit the excess noise, giving Eve extra information above the BS attack. We show statistical fluctuations (± 1 standard deviation) corresponding to a data subset of 5000 points per block, as on Fig. 3.

We find that the Gaussian mutual information I_{AB}^g is lower than the actual mutual information I_{AB}^{ng} , with a very small gap between them ($\leq 0.8\%$ for modulation of $V_A = 36.6 N_0$) for any T and ϵ . Therefore, only the curve I_{AB}^g (noted I_{AB}) has been represented on Fig. 5.

On Eve's side, Fig. 5 compares I_{AB} with three possible values of I_{BE} . The dotted line (I_{BE}^{BS}) is obtained from a BS attack for the given transmission. With this attack, Eve only makes use of the channel losses, as if she was not able to exploit the excess noise. The dashed line ($I_{BE}^{partial IR}$) is obtained when, in addition to the BS attack, Eve exploits the excess noise for implementing a partial IR attack. This information therefore reads

$$I_{BE}^{partial IR} = \mu I_{BE}^{IR} + (1 - \mu) I_{BE}^{BS}, \quad (3)$$

The experimental points shown over the dashed line are obtained from this formula, using the measured information acquired by Eve from the IR part of the attack I_{BE}^{IR} , and the evaluated information from the BS attack (dotted line). The solid line (I_{BE}^g) is the optimal Gaussian attack where Eve exploits the excess noise for implementing an entangling cloner attack. The experimental points shown over this solid line are the bounds on I_{BE} deduced from the measured line parameters, according to eq. 2. These curves show the crucial role of the excess noise,

even if Eve does not implement the strongest attack. On Fig. 5 one can actually read the tolerable excess noise for a given channel transmission T , at the crossing point between I_{AB} and I_{BE} , confirming that Alice and Bob are on the “safe side” when using the Gaussian bound [7].

In conclusion, we have implemented a family of quantum attacks, namely partial intercept-resend attacks, which allow Eve to exploit the excess noise and are thus more general than simple “beam-splitting attacks” as considered so far. Our experiment confirms that such attacks can be successfully detected and eliminated by accurately monitoring the variances of all (“vacuum” and “excess”) noises of the channel. Therefore, the present “real-case study” provides both a test and an illustration of the working principles of experimental CV-QKD. It is also particularly important in view of the recent proof [14, 15] that the optimal *collective* attack for a given noise variance is Gaussian, just as for individual attacks. Considering that our family of attacks spans all possible relevant transmissions and noise variances of the channel, the security of our Gaussian-modulated protocol remains warranted under very general conditions.

We acknowledge financial support from the EU under projects COVAQIAL (FP6-511004) and SECOQC (IST-2002-506813), and from the IUAP programme of the Belgian government under grant V-18. R.G-P. acknowledges support from the Belgian foundation FRiA.

-
- [1] Nicolas Gisin, Grégoire Ribordy, Wolfgang Tittel, and Hugo Zbinden. Quantum cryptography. *Rev. Mod. Phys.*, 74:145–195, 2002.
 - [2] Mark Hillery. Quantum cryptography with squeezed states. *Phys. Rev. A*, 61:022309, 2000.
 - [3] T. C. Ralph. Continuous variable quantum cryptography. *Phys. Rev. A*, 61:010303, 2000.
 - [4] Frédéric Grosshans, Gilles Van Assche, Jérôme Wenger, Rosa Brouri, Nicolas Cerf, and Philippe Grangier. Quantum key distribution using gaussian-modulated coherent states. *Nature*, 421:238–241, 2003.
 - [5] Frédéric Grosshans, Nicolas J. Cerf, Jérôme Wenger, Rosa Tualle-Brouri, and Philippe Grangier. Virtual entanglement and reconciliation protocols for quantum cryptography with continuous variable. *Quantum Information and Computation*, 3:535–552, 2003, Special Issue.
 - [6] Ryo Namiki and Takuya Hirano. Security of continuous-variable quantum cryptography using coherent states: Decline of postselection advantage. *Phys. Rev. A*, 72:024301, 2005.
 - [7] Frédéric Grosshans and Nicolas J. Cerf. Continuous-variable quantum cryptography is secure against non-gaussian attacks. *Phys. Rev. Lett.*, 92:047905, 2004.
 - [8] Gilles Van Assche, Jean Cardinal, and Nicolas J. Cerf. Reconciliation of a quantum-distributed gaussian key. *IEEE Trans. Inform. Theory*, 50(2):394–400, 2004.
 - [9] Matthieu Bloch, Andrew Thangaraj, and Steven W. McLaughlin. Efficient reconciliation of correlated continuous random variables using ldpc codes. 2005.

- [10] Jérôme Lodewyck, Thierry Debuisschert, Rosa Tualle-Broui, and Philippe Grangier. Controlling excess noise in fiber-optics continuous-variable quantum key distribution. *Phys. Rev. A*, 72:050303(R), 2005.
- [11] Frédéric Grosshans. Collective attacks and unconditional security in continuous variable quantum key distribution. *Phys. Rev. Lett.*, 94:020504, 2005.
- [12] Miguel Navascués and Antonio Acín. Security bounds for continuous variables quantum key distribution. *Phys. Rev. Lett.*, 94:020505, 2005.
- [13] Johannes Rigas, Otfried Gühne, and Norbert Lütkenhaus. Entanglement verification for quantum-key-distribution systems with an underlying bipartite qubit-mode structure. *Phys. Rev. A*, 73:012341, 2006.
- [14] R. Garcia-Patron and N. J. Cerf. Unconditional optimality of gaussian attacks against continuous-variable qkd. *Phys. Rev. Lett.*, 97:190503, 2006.
- [15] M. Navascues, F. Grosshans, and A Acín. Optimality of gaussian attacks in continuous variable quantum cryptography. *Phys. Rev. Lett.*, 97:190502, 2006.